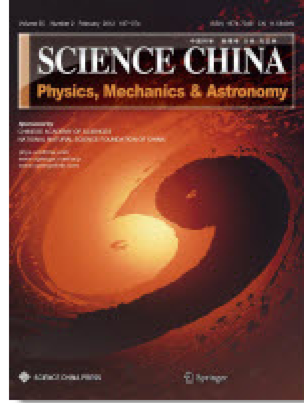

Characterization and removal of contaminants in lithography

Journal:	*SCIENCE CHINA Physics, Mechanics & Astronomy*
Manuscript ID	SCPMA-2024-0712.R2
Manuscript Type:	Review
Date Submitted by the Author:	16-Oct-2024
Complete List of Authors:	Gao, Yawen Chen, Changsheng; Tsinghua University Wang, Feng Li, Mingbo; Shanghai Jiao Tong University Sun, Chao; Tsinghua University, Department of Energy and Power Engineering and Department of Engineering Mechanics
Keywords:	photolithography, immersion fluid, contamination, droplet, bubble, particle
Speciality:	Fluid Dynamics
Note: The following files were submitted by the author for peer review, but cannot be converted to PDF. You must view these files (e.g. movies) online.	
Manuscript-Latex.zip	

SCHOLARONE™
Manuscripts

1
2
3
4
5
6
7
8
9
10
11
12
13
14
15
16
17
18
19
20
21
22
23
24
25
26
27
28
29
30
31
32
33
34
35
36
37
38
39
40
41
42
43
44
45
46
47
48
49
50
51
52
53
54
55
56
57
58
59
60

SCIENCE CHINA
Physics, Mechanics & Astronomy

• Review Article •

October 2024 Vol. No.:
https://doi.org/

Characterization and removal of contaminants in lithography

Yawen Gao[1], Changsheng Chen[1], Feng Wang[1], Mingbo Li[2], and Chao Sun[1,3*]

[1]New Cornerstone Science Laboratory, Center for Combustion Energy, Key Laboratory for Thermal Science and Power Engineering of Ministry of Education, Department of Energy and Power Engineering, Tsinghua University, Beijing 100084, China;
[2]Key Laboratory of Hydrodynamics (Ministry of Education), School of Ocean and Civil Engineering, Shanghai Jiao Tong University, Shanghai 200240, China;
[3]Department of Engineering Mechanics, School of Aerospace Engineering, Tsinghua University, Beijing 100084, China

Received ; accepted

Photolithography is a foundational technique for manufacture compact chips in semiconductor industries. Regulating and cleaning contaminants in lithographic processes are crucial for achieving the higher resolution and smaller feature sizes, which contain a variety of physical phenomena related to fluid dynamics. In this review, we will first introduce the basic principles of two mainstream lithography, namely deep ultraviolet (DUV) lithography and extreme ultraviolet (EUV) lithography. We critically review several types of contaminants such as droplets, bubbles, particles and chemical organic pollutants, highlighting the advanced techniques for identifying the nano-substances and fluid behaviours. Then the control strategies for mitigating contaminants are reviewed, especially for the contamination removal on photomask, the improvement on the purity of immersion liquid and efficient cleaning treatment for wafer surface. This review underscores the critical need for advanced contaminant management strategies in photolithography, integrating innovative cleaning techniques that promise to elevate lithographic performance and drive future developments in semiconductor technology.

photolithography, immersion fluid, contamination, droplet, bubble, particle

PACS number(s): 48.20.Ky, 47.61.Jd, 47.55.-t, 85.40.HP

Citation: Gao Y W, Chen C S et al, Characterization and removal of contaminants in lithography, Sci. China-Phys. Mech. Astron. , (2024), https://doi.org/

For Review Only

1 Introduction

The rapid progress in the semiconductor, electronic and information industries has shone a spotlight on the high-resolution lithography [1], which pursuits the dual goals of lower power consumption and higher performance [2]. The ongoing evolution of optical lithography technologies is driven by the Moore's law [3], an empirical relation that predicted a doubling of the number of integrated circuits on a microchip every 18-24 month [4]. With the explosive growth of artificial intelligence and data-driven applications, the continuation of Moore's Law in the coming decades is imperative to support the increasing demand for computing power and data storage [5].

Basically, optical lithography leverages the photochemical sensitivity of photoresist under the exposure to visible light, ultraviolet light or electron beam to facilitate the transfer of graphical circuit patterns from a mask to a wafer [6]. Thereby, the main approaches to improve the resolution of optical lithography lie in the decrease of the wavelength of incident light [7], the increase of numerical aperture [8], and reduction of the process factors by the use of optical techniques, such as phase shifting masks or off-axis illumination. To address the demand for higher resolution and smaller feature sizes, various next-generation lithogra-

*Corresponding author (email: chaosun@tsinghua.edu.cn)

© Science China Press and Springer-Verlag GmbH Germany, part of Springer Nature 2020

1
2
3
4
5
6
7
8
9
10
11
12
13
14
15
16
17
18
19
20
21
22
23
24
25
26
27
28
29
30
31
32
33
34
35
36
37
38
39
40
41
42
43
44
45
46
47
48
49
50
51
52
53
54
55
56
57
58
59
60

phy technologies have been developed, including immersion lithography, extreme ultraviolet (EUV) lithography, electron beam direct-write (EBDW), imprint lithography (IL), and ion-projection lithography (IPL). The adoption and evolution of these technologies depend on their ability to balance performance benefits with considerations of cost, efficiency, and integration challenges within established manufacturing ecosystems.

However, with the improvement of chip integration and the decrease of the light source's wavelength, the contamination issues become more pronounced [9]. In the photolithography process, contaminants, manifesting as droplets, bubbles and particles, pose a risk of infiltration at every stage. They may originate in the laser source chamber [10], the intermediate medium and the photoresist, potentially impacting the integrity of the final product. This review will begin with a concise overview of optical lithography, followed by a detailed discussion of potential contaminants encountered in photolithography. In addition, emphasis is placed on the detection methods and cleaning techniques that have been adopted. The purpose of this review is to help the researchers understand the problems of characterization and removal of contaminants in immersion lithography and provide better control approaches for the improvement of exposure performance .

For Review Only

2 General overview of photolithography

Lithography is a fundamental method for mass production of integrated circuits in the semiconductor industry. It is essential in the fabrication of microprocessors, memory chips, and various electronic components. Normally, lithography process has several steps and the position of each components are shown in Figure 1(a) [11]. A silicon wafer is cleaned with the free of dust, contaminants and chemical residues. A light-sensitive photoresist is dropped on surface of the wafer through a technique called spin coating. Then the wafer, aligned with a photomask with the desired circuit pattern, is exposed to light (usually ultraviolet), which selectively softens the photoresist (positive) where light passes through the transparent areas of the mask. After exposure, the wafer undergoes a development process where the soft photoresist is washed away, revealing the substrate in the pattern defined by the mask [12]. The uncovered substrate are then etched away using chemical or plasma etching techniques [13]. Upon the completion of the etching process, the residual photoresist is removed and uncovering the etched patterns, showing the intended circuits or structures.

The resolution limit of the optical expose system R is fundamentally constrained by diffraction, typically described by the Rayleigh criterion [14]:

$$R = k_1 \times \frac{\lambda}{NA} \tag{1}$$

where k_1 is the process factor, λ is the wavelength, and NA is the numerical aperture of the imaging system. Enhancements in lithographic resolution can be achieved by using short wavelength of the light source, decreasing the process factor, or increasing the numerical aperture of the projection lens. Another key parameter in chip manufacture is depth of focus (DOF):

$$DOF = k_2 \times \frac{n\lambda}{NA^2} \tag{2}$$

where n is the index of refraction, and k_2 is process factor. A larger DOF value means the longer clear distance for etching with a better lithography quality. Driven by scientific advancements, the current technology node (resolution) of lithography has progressed to below 5 nm [15]. Although the next generation of lithography technology using new principles is continuing to extend, the mainstream lithography technology currently and even in the future for a long time to be applied in the commercial field still relies on deep ultraviolet lithography and extreme ultraviolet lithography technology.

2.1 Deep ultraviolet lithography

Deep ultraviolet (DUV) lithography is a well-established technology that has found extensive application in the fabrication of integrated circuits, microelectromechanical systems (MEMS), and other micro-nano manufacturing domains. According to the International Roadmap for Semiconductors (ITRS), the lithography technology cycle progresses every three years, with current advancements primarily concentrated on DUV immersion lithography operating at a wavelength of 193 nm, EUV lithography at 13.5 nm, and other emerging technologies. Interestingly, DUV lithography has dominated the field much longer than initially expected, with a continual series of improvements extending its lifespan [16].

Immersion lithography is an improved technology of DUV lithography, which aims to increase the numerical aperture that is etched onto silicon wafers [17]. The working principle is shown in Figure 1(b). It increases the NA upon traditional photolithography by filling the space between the lens and the wafer with water (1.44 versus 1.0 for air), thereby improving the lithography resolution [18-20]. The coupled effect of the short wavelength and the higher NA enabled by the immersion fluid allows for patterning smaller feature sizes and advanced technique nodes.

However, immersion lithography introduces several challenges that affect the exposure performance of the system.

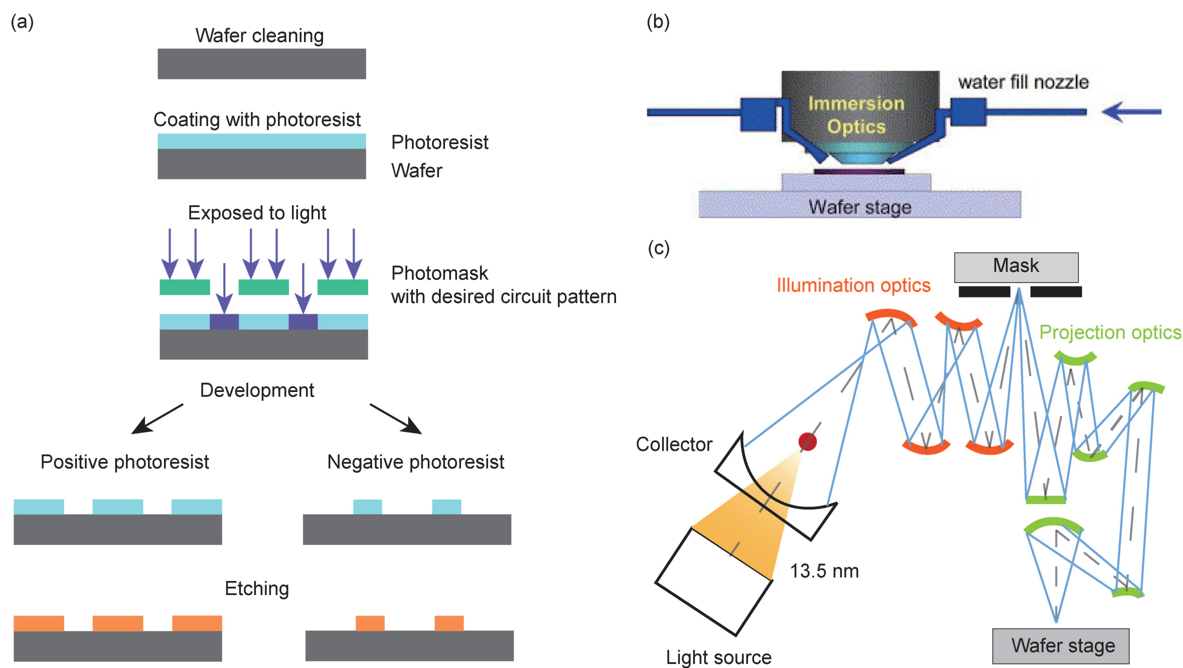

Figure 1 (a) Basic principle of photolithography process [12]. (b) Schematic of immersion lithography. Permission is from [18]. (c) Schematic of an EUVL set up operated in the vacuum environment [24, 25].

Contact line instabilities may occur during the high-speed relative motion of the lens and the wafer [21], entraining bubbles at the advancing contact line and releasing droplets at the receding contact line. The presence of bubble may distort the light path, significantly influencing the accuracy. Uneven drying of the water on the wafer can result in "water marks," leading to further defects [22]. These defects not only directly diminish the manufacturing yield of chips but also pose a risk by inducing the contamination to the immersion head, indirectly affecting both yield and production costs.

Due to the higher requirement on the feature size on silicon wafer, immersion lithography has played a pivotal role in enabling these advancements, particularly for critical layers of chips with nodes at 45 nm and below. At present, the 193 nm immersion lithography machine has been the mainstream technology in fabs, relying on multiple exposure technology to achieve the production of 32 nm memory devices, 20 nm, 14 nm and even smaller logic devices. However, as the semiconductor industry pushes towards even smaller geometries, below 10 nm, techniques like EUV are beginning to complement or even replace immersion lithography for the most critical layers. Nonetheless, immersion lithography remains a key technology in the semiconductor manufacturing process for numerous less critical layers and for nodes where EUV is not yet cost-effective.

2.2 Extreme ultraviolet lithography

Although the actual application is nearly 10 years later than originally estimated, EUVL is the most advanced lithography technology. ASML in the Netherlands is the only supplier for the production of EUVL machines. Its working principle is shown in Figure 1(c) [23-25]. EUV light is synthetically produced within a light source cavity, where a tin (Sn) droplet is illuminated by a high-energy plasma generated from a high-power laser shot in a vacuum, emitting light at 13.5 nm wavelength in all directions [26]. A collector mirror focuses the light into a reflective optical system that directs the light onto a reticle stage containing patterns. EUV beam reflected by the mask is subsequently focused by a second set of mirrors (projection optics) onto the wafer stage, where it prints a pattern onto a photoresist-coated wafer surface.

EUV lithography is conducted under near-vacuum conditions to minimize the absorption of EUV light with short-wavelength. Within the light source cavity, solid particles from component degradation or external contaminants can accumulate on mirrors and optical surfaces, potentially causing defects in semiconductor products. Additionally, degassing from materials such as photoresist in vacuum enables to create chemical films, which can absorb EUV light, thus reducing system efficiency and damaging critical components.

With the further reduction of the feature size of integrated circuits, even to the present 3 nm node, it is quite important to regulate the contamination issues. Apart from the contaminants generated in the laser source chamber [10], the purity

Review Only

1 2 3 4 5 6 7 8 9 10 11 12 13 14 15 16 17 18 19 20 21 22 23 24 25 26 27 28 29 30 31 32 33 34 35 36 37 38 39 40 41 42 43 44 45 46 47 48 49 50 51 52 53 54 55 56 57 58 59 60

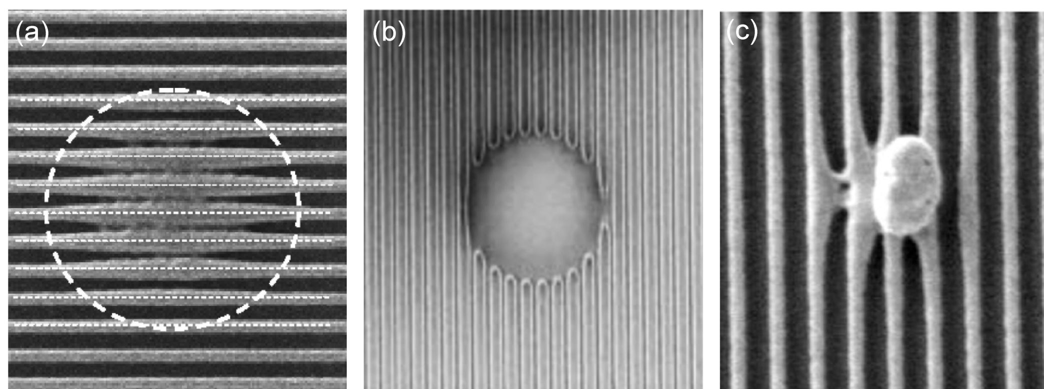

Figure 2 Defects caused by contamination of (a) water droplets after evaporation [29], (b) trapped bubbles [19] and (c) particles [30]. Images were captured by scanning electron microscope (SEM). The pitch between two lines in (a) is 220 nm. Size of the bubble in (b) is 3 μm. Particle affecting pattern in (c) is 0.1–5 µm.

For Review Only

of photoresist determines the integrity of the final product as well. Contaminants incorporated into the film layer during the etching process, such as carbon, oxidative and detrital pollution can compromise both the quality and the composition of the chip [27, 28].

3 Potential contaminants and detection techniques in lithography

Many published works point out that although immersion lithography has been widely used, the use of immerse liquid is easy to induce contaminants in exposure optics, compared to dry lithography. Figure 2 illustrates the typical exposure defects on a wafer caused by contaminants of water droplet, bubble and particle. Local heat and stress affect the uniformity of the immersion flow field, resulting in the variation of the refractive index and reducing the quality of the exposure environment.

From the practical scenario, the exchange of substances in the immersion flow field is depicted in Figure 3(a). With the scanning of the laser, water and photoresist interact, resulting in permeation and extraction processes. To minimize light reflection, a bottom anti-reflective coating (BARC) is applied beneath the photoresist. Within the exposure area, the laser and impurities can potentially form cavitation air bubbles and particles, negatively impacting resist imaging. Additionally, a temperature gradient causes water on the resist surface to evaporate as the bottom stage moves. Residual water droplets may interact with the external environment, leading to interfacial phenomena on the surface profile, such as precipitation, staining, and defect formation [22].

From the theoretical scenario, these interfacial phenomena compass a range of physical processes. From the macroscopic side, scaling analysis is a powerful tool to discern how various physical parameters affect the system. Several dimensionless numbers are commonly used to characterize the interfacial phenomena [31], including Weber number (W_e), Reynolds number (R_e), Capillary number (C_a), Bond number (B_o), Marangoni number (M_a), which give comprehensive descriptions of the role of inertia, surface tension, viscosity, gravity and surface tension gradient. Utilizing these dimensionless numbers allows for substantial simplification of the Navier-Stokes equations, facilitating the interfacial challenges, such as those exemplified by Stokes flow and the lubrication approximation. On the microscopic scale, the molecular kinetic theory (MKT) offers novel perspectives on the contact line hydrodynamics, including thermal fluctuations [32]. This theory has been proposed to address the paradox of the moving contact line. For substrates with physical defects, the pinning-supersaturation mechanism [33, 34] governs the stability of surface nanobubbles, such as $\sin\theta_e = \zeta L/L_c$, where ζ is the gas supersaturation, L and L_c are the footprint and critical lateral extension under ambient condition, respectively. Since contaminants are prone to adsorb at the substrate, particularly along the contact line, they can also affect the pinning force f_{pin}, which, in turn, modulates the de-pinning and re-pinning behaviors of the contact line. Typically, when the pinning force f_{pin} exceeds the difference $\cos\theta - \cos\theta_Y$, where θ_Y is Young's angle, depinning occurs; otherwise, the system exhibits pinning.

This section primarily introduces various contaminants in the immersion flow field and reviews relevant studies addressing interfacial phenomena and detection methods. It aims to provide a comprehensive understanding of contamination issues and highlight ongoing research efforts.

3.1 Droplet

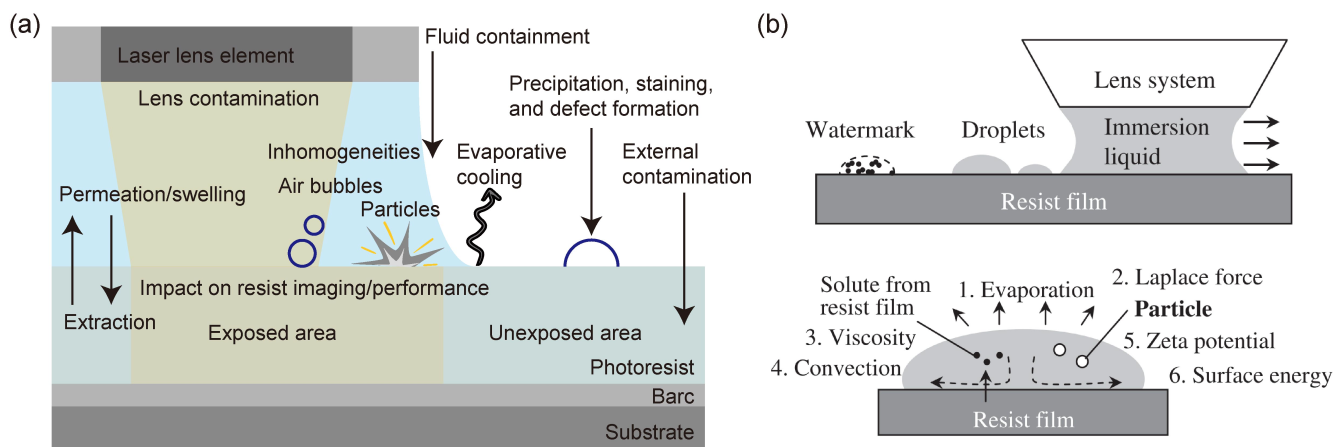

Figure 3 (a) Interaction of components in immersion lithography. Reprinted with permission from the work [22]. (b) Formation of watermarks on the resist surface. Permission is obtained from [40].

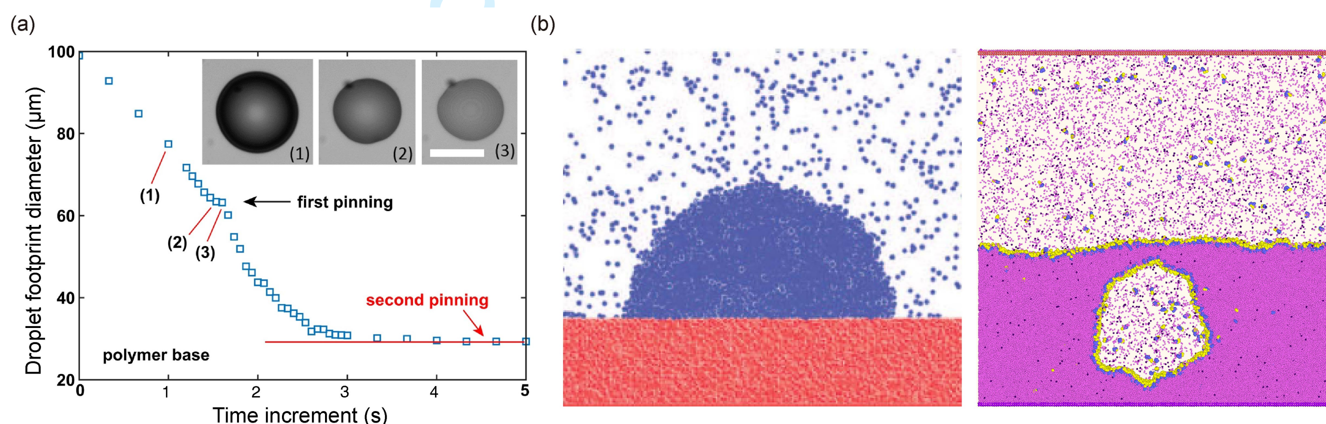

Figure 4 (a) Time evolution of the droplet footprint diameter during evaporation on a DUV photoresist surface. Initial diameter is 800 μm. Inset: droplet top-view images corresponding to the three labeled points. The white scale bar corresponds to 50 μm [41]. (b) Molecular dynamics simulation of a droplet on a substrate [44] and a nanobubble stabilized by surfactant molecular in the bulk. Left: blue particles are liquid atoms, red particles are solid atoms. Contact angle is 90 °. Right: white area is gas phase, and pink dots are solvent. Yellow and blue dots represent the hydrophobic tail and hydrophilic head of surfactant.

Droplet contaminants always result from the hydrodynamic instabilities, especially at the receding contact line in immersion lithography [21]. The partial loss of the immersion liquid is unacceptable for the further development of high-resolution lithography. To understand the instability of the moving contact line, the fundamental physical process of high-speed droplet impact has been intensively investigated [35-37]. Snoeijer & Andreotti comprehensively discussed the movement of the three-phase contact line, tightly connecting the macroscopic motion with the microscopic processes [32]. Xu et al. [38] studied the influence of surrounding gas pressure on the splashing of an impacted droplets, highlighting the compressible effects in the gas phase on the contact line stability. Thoroddsen et al. [39] experimentally observed the bubble entrapment during the drop impacting onto a solid surface, which may also occur during the high-speed motion of the immersion liquids [21].

The subsequent evaporation process of the droplet contaminants can lead to more damages to the lithography process. Niiyama et al. [40] reported on the dynamic formation of drying stains, as illustrated in Figure 3(b). Drying stains are formed because of the deposition of contaminants during the evaporation of droplets, a phenomenon commonly referred to as the ”coffee ring effect”. Watermark of liquid containing particles were formed at the center of the droplet in a ring shape, driven by the Laplace force and pinning effect. Sufficient evaporation of water droplets can significantly reduce the formation of stains and watermarks on wafers [41]. Diameter of droplet decreases during evaporation, accompanied by two instances of pinning behavior, as shown in Figure 4(a).

When the droplet is composed of multiple components, the evaporation dynamics becomes much more complicated, due to the intrinsic interplay among fluid flow, heat transfer and mass transport [31]. The physio-chemistry parameters in-

1 2 3 4 5 6 7 8 9 10 11 12 13 14 15 16 17 18 19 20 21 22 23 24 25 26 27 28 29 30 31 32 33 34 35 36 37 38 39 40 41 42 43 44 45 46 47 48 49 50 51 52 53 54 55 56 57 58 59 60

volve the Laplace force, viscosity, the inside convection of droplet, zeta potential and surface energy. In this context, Wakata et al. [42] utilized both the high-speed imaging and the infrared imaging techniques to investigate the evaporation dynamics of water-ethanol droplets in an acoustic levitation field. Combining the theoretical models and numerical simulations, the volume and concentration evolution of droplets are well predicted. Furthermore, Zeng et al. [43] investigated the evaporation dynamics of ternary mixture droplets, where the selective evaporation and phase separation processes produce rich physical phenomena.

In the field of nanoscale fluid dynamics, molecular dynamics (MD) simulation is a powerful tool for investigating the wetting, spreading, and evaporation of nanodroplets. In-situ (non-invasive) dynamic observation of droplets at the microscopic scale, coupled with the measurement of microscopic physical quantities, is challenging to achieve through experiments alone. Combining MD simulations with experimental methods aids in studying the dynamic behavior of droplets, particularly the movement of contact lines during evaporation and the laws governing motion in the DUV immersion flow field. In Figure 4(b), an MD model was built to simulate the stability of a droplet on a substrate [44]. Chen et al. [45] investigated the multi-interaction between gas bubble, surfactant and water phase via MD simulation. After 100 ns, gas is still existed, stabilizing by contaminant (surfactant molecules). MD simulation is a potential approach to figure out the dynamic behaviour of droplet and bubble in the immersion field under the mimic environment of lithography. Yang et al. [46] conducted experimental research on water condensation and evaporation at the sub-nanometer scale, deviating from the classical Kelvin equation, providing valuable insights for researchers studying droplet motion at the nanoscale. Similarly, Seveno [47], Wu [48], Zhang [49], and Tasao [50], among others, have explored the dynamic behaviors of the contact line and contact angle of droplets at the microscopic level using MD simulations. Therefore, MD simulation is a promising tool for studying the dynamic behavior of water droplets during evaporation in immersion lithography.

3.2 Bubble

Bubbles can form within liquid containment systems due to the devolution of dissolved gas and cavitation effects [30]. The presence of air bubbles within the immersion layer can significantly degrade image quality, as the introduction of inhomogeneity bubbles causes an index of refraction discontinuity and light scattering along the optical path. There are several works highlighted the controllable strategies of bubbles in lithography process. Akira Kawai et al. [51] employed an atomic force microscope (AFM) to characterize nanobubbles on the resist surface immersed in distilled water, demonstrating that nanobubbles can be manipulated using an AFM tip. Moreover, performing the Mie theory and finite-difference time-domain (FDTD) simulation, Lin et al. [52] discovered that when the diameter of a bubble exceeds 90 nm, the light scattering properties substantially affect image quality in immersion lithography. The impact is even more pronounced when the bubble is positioned on the resist surface. Conversely, Burnett et al. [53] reported that no air entrainment was observed under a mimic velocity and a contact angle of immersion lithography. Hydrophobic surface has high possibility to trap bubbles than the hydrophilic. However, a hydrophilic surface can exhibit hydrophobic-like behavior when the velocity of the free surface reaches a certain high value.

In the past two decades, bulk nanobubbles have attracted wide interest from academia to industry due to a series of unique properties, especially their exceptional stability. Typically, the hydrodynamic diameters range between 50 nm and 200 nm [54-56]. Their enduring stability, often lasting from days to weeks, has been consistently characterized through various sophisticated detection methods such as light scattering, dark field imaging, and cryo-transmission electron microscopy [57-59]. In immersion flow field, nanobubbles are difficult to be removed and can potentially affect exposure and imaging. There are several alternatives to characterize such nanoscale matters.

Nanoparticle tracking analysis (NTA) is an advanced technique to measure the size distribution, motion trajectory, and number density of nano-substances in the liquid, as shown in Figure 5(a) [60, 61]. Bubbles in suspension scatter the laser light, making them visible as points of light moving under Brownian motion. The rate of bubble movement is influenced by bubble size, as described by the Stokes-Einstein equation, which links the diffusion coefficient to the size of the bubble. The recommended concentration of sample for NTA measurement is between 10^6 and 10^9 particles/mL, and the lowest detected limit on diameter is 20 nm. At the same time, Li et al. [62, 63] investigated the nucleation and stability of bulk nanobubbles in aqueous solution under varying pH levels, ionic-surfactant concentrations, ionic strengths and temperatures, by applying coupled techniques of NTA and dynamic light scattering (DLS). They explored how bulk nanobubbles respond to temperature changes and observed that nanobubbles can expand and contract reversibly as the temperature varies (Figure 5(b)). The intricate balance of competing interactions between water self-ionization and mobility of ions on the surface dominates this dynamic phenomenon. Enhanced stability of nanobubbles in aqueous solutions can be attributed to the effective accumulation of net charges, as

For Review Only

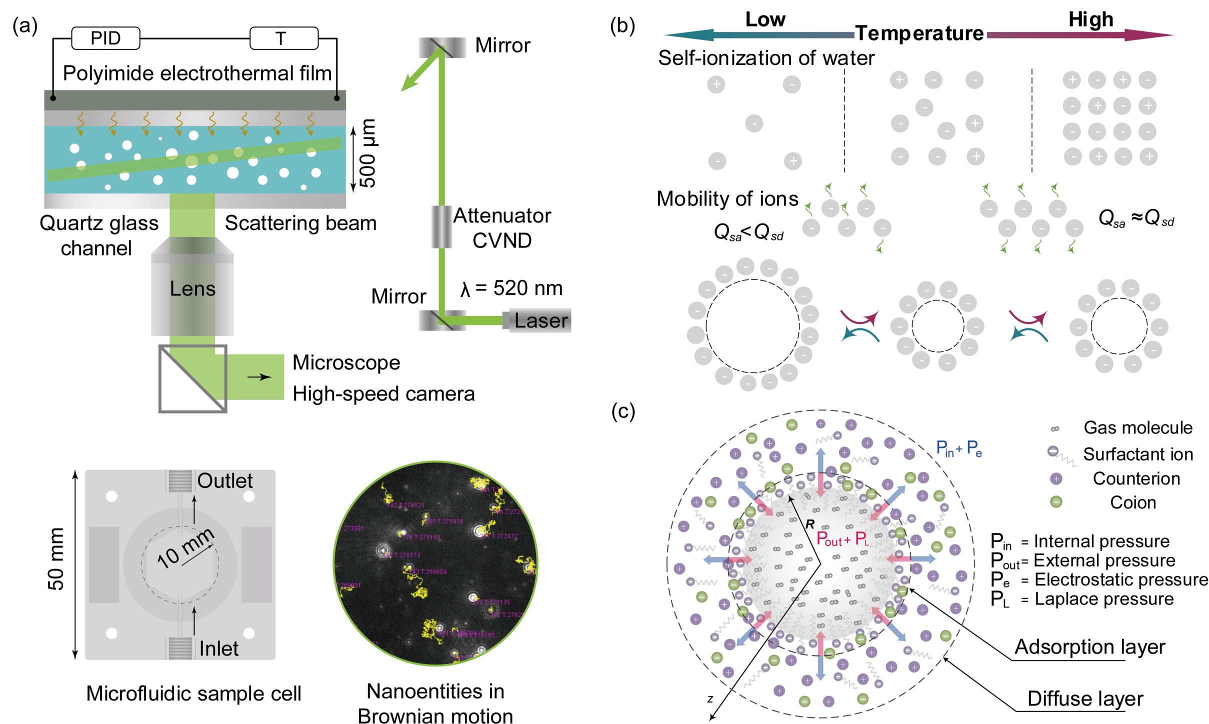

Figure 5 (a) Schematic illustration of the NTA system (not-to-scale) used for the 'direct' imaging of nanoscale entities. The lower-left shows the top view of the microfluidic sample cell. The lower-right shows the trajectories of the nanoentities doing Brownian motion in the field of vision [61]. (b) Schematic diagram illustrating the physical processes responsible for the effect of temperature on the ion accumulation and further the equilibrium size of the bulk nanobubble. Under the influence of temperature, competition between the water ionization and ion mobility determines the net amount of charges on the bubble surface [63]. (c) Schematics of the adsorption layer structure of ions and surfactants surrounding a negatively charged bulk nanobubble [62].

shown in Figure 5(c). However, there are still discrepancies between the theoretical predictions by the ion stabilization model and experimental results, indicating that current comparison still has shortcomings.

DLS is also a powerful technique for analysis of the nanosubstances. The size of the particle is determined by the fluctuations in scattered light intensity due to the Brownian motion [60]. It is important to note that NTA and DLS cannot distinguish between substances in the immersion liquid such as particles, bubbles and aggregates [64]. These theoretical and experimental studies provide pioneering ideas for characterizing of nano-entities in fluid fields, which is helpful for understanding the formation and stability of bulk bubbles in submerged flow, thus enhancing the efficiency and quality of the imaging process [65].

The existence of surface nanobubbles has been explained by the pinning-gas supersaturation mechanisms [21, 33, 34, 66]. In photolithography process, exposed photoresist involves in photo-chemical reactions, while the area protected by the mask remained unchanged. Such inhomogeneous solid-liquid interfaces encourage the pinning effect on the photoresist surface. In addition, the heat released from these reactions causes local gas supersaturation in the submerged flow field, creating ideal conditions for the formation and stability of surface nanobubbles. Despite ongoing controversy about the existence of bulk nanobubbles [67-69], experimental evidence suggests that some nanoentities observed are indeed bubbles [70, 71]. MD simulation indicates that under certain conditions, both bulk nanobubbles and surface nanobubbles can form and remain stable for a long time [72, 73]. Xiao et al. [74] investigated the destabilization mechanism of surface nanobubbles at the molecular level by MD. These insights imply that as long as the flow field is controlled out of the stable condition, the negative effect from nanobubbles on the lithography can be eliminated.

3.3 Particle

Particles are ubiquitous contaminants in immersion lithography, originating from various sources such as air, chemicals, photoresist, and even the silicon wafer itself. These contaminants compromise the overlay and focus accuracy, critical parameters in lithographic quality. Additionally, a secondary pollution issue arises in the immersion liquid due to particles peeling off from the overflow substrate, further complicating the contamination challenges in the technique.

The existence of leaching contaminants can change the refraction index and reduce the optical transmission. Particles

may be carried by water flow to the lens surface and accumulate at surroundings [19]. Furthermore, Terai reported that the low adhesion between wafer bevel and coated film on the resist may lead to the film peeling [75]. As the exposure progresses, particles can be transported back and forth by the flow from the wafer edge to the wafer center. The geometry of wafer edge affects the defectivity performance in ArF immersion lithography. Tamura et al. [76] reported that long edge wafer has less number of bridging defects than the short edge, while the particles or flakes after coating are easy to be peeled off on the short-edge wafer. To mitigate undesirable interactions between water and photoresist, it has been proposed to apply a top coat material onto the photoresist film, thereby eliminating direct contact between the water and the photoresist. Takahashi et al. [77] revealed particles contaminating the topcoat can be vertically transferred onto the surface of resist. DLS and contact angle meters were used to evaluate the particle size and hydrophilicity of underlying substrate. The rate of particle transfer to the resist pattern can be minimized by controlling the surface voltage of the resist.

3.4 Chemical contamination

Organic contamination in immersion lithography mainly comes from the photoresist and its adhesive materials. Interactions of water-photoresist may lead to the leaching of the photoresist components and the alteration of the photoresist composition, further deteriorating the photoresist pattern profile. Photo-acid generators (PAGs), as a resultant component after extraction, is one of the causes for defects formation in immersion lithography. Furthermore, the extraction products contaminate the water itself, thus decreasing the transmittance and corroding the lens [78]. To monitor the concentration and temporal evolution of chemical contaminants in the immersion flow field of lithography, Sado et al. [79] conducted comprehensive measurements on the immersion field, resist and wafer. Their study characterized various features of contaminants, such as size, shape, configuration, components and concentration.

The extraction of photoresist into water can be analyzed using advanced techniques such as liquid chromatography–mass spectrometry (LC–MS), X-ray photoelectron spectroscopy (XPS) and time-of-flight secondary ion mass spectrometry (TOF-SIMS). These techniques allow for detailed chemical analysis and identification of chemical contaminants at very low concentrations. LC-MS, for example, combines the physical separation capabilities of liquid chromatography with the mass analysis capabilities of mass spectrometry, making it highly effective for detecting and quantifying organic compounds in photoresists. XPS provides elemental composition information and chemical state information from the surfaces of materials, while TOF-SIMS offers high-resolution surface analysis, capable of detecting and mapping the distribution of contaminants at the molecular level. Figure 6 illustrates the features of these contamination detection approaches.

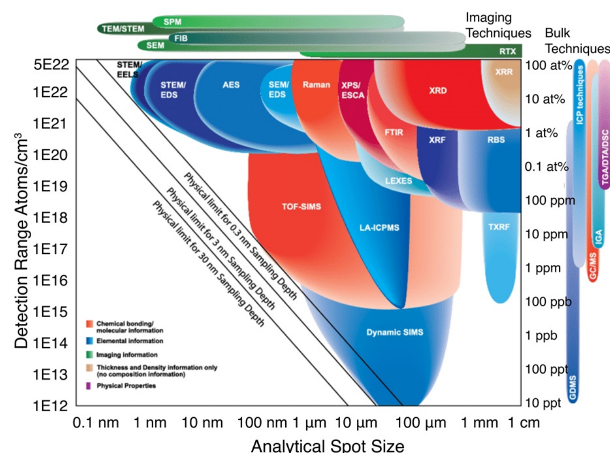

Figure 6 Bubble chart of the resolution for analytical methods as the function of detection limit [80].

Dynamic secondary ion mass spectrometry (SIMS) offers the highest resolution for surface detection among these techniques. It is particularly useful for depth profiling, allowing researchers to study the distribution of contaminants and dopants throughout the photoresist layers. On the other hand, energy dispersive X-ray (EDX) spectroscopy is used to identify specific wafer defects. EDX, often coupled with scanning electron microscopy (SEM), provides information on the elemental composition of defects, helping to trace their origin and understand the formation mechanisms [81].

Furthermore, Chi et al. [82] developed a laser ablation inductively coupled plasma mass spectrometry (ICP-MS) method for determining impurities in viscous photoresist, including elements such as aluminum (Al), copper (Cu), platinum (Pt), gold (Au), thorium (Th), and uranium (U). This technique involves using a laser to vaporize a small portion of the sample, which is then analyzed by ICP-MS for its elemental composition. ICP-MS is renowned for its sensitivity and precision, making it ideal for detecting trace levels of metal contaminants. It is designed to assess the quality of G-line photoresist, meeting a stringent quality requirement of 200 ng/mL. Ensuring low levels of metal impurities is critical as it can affect the electrical properties and reliability of the final semiconductor devices.

Kusumoto et al. [78] employed LC-MS to detect the composition of leached materials, including the photoacid generator (PAG) and its decomposition products. The leaching amount was found to be on the order of 10^{-12} mol/cm^2. PAGs are crucial components in chemically amplified resists used

For Review Only

in modern lithography, where they generate acid upon exposure to light, initiating the deprotection reaction in the photoresist. The stability and purity of PAGs are vital for the performance of photoresists, as impurities can lead to undesired reactions and affect the resolution and line edge roughness of the printed patterns.

In addition to these detection methods, the field is also exploring innovative cleaning techniques to reduce the presence of contaminants. Methods such as megasonic cleaning [83], which uses high-frequency sound waves to remove particles from surfaces, and jet spray cleaning, which employs high-pressure liquid jets, are being optimized for use in lithography. Aerosol cleaning, which involves the use of fine mist to clean surfaces, is another promising approach.

The integration of these advanced analytical techniques with rigorous cleaning protocols and material engineering is essential for advancing immersion lithography. As the industry pushes towards smaller feature sizes and higher device densities, the control of contaminants will remain a critical challenge. Continuous research and development in this area are necessary to ensure the reliability and performance of future semiconductor devices.

4 The removal of contaminants

Contamination control is particularly important in lithography, as pattern defects introduced during exposure are transferred to the wafer, compromising the entire process. Effective contamination control methods are essential to maintaining the integrity of the lithographic process, improving yield rates and reducing production costs by preventing issues such as haze formation, particle deposition and chemical residues.

Currently, several techniques are employed to remove contaminants from critical areas. These include pressurization, inert gas purging, the use of chemical reagents, and electric grounding [84]. Each of these methods addresses specific contamination challenges and contributes to overall process cleanliness.

Special attention should be directly towards the control of contaminants affecting the photomask, projection lens, immersion liquid and wafer surface. The photomask, which contains the pattern to be transferred, necessitates free from particles and residues to guarantee precise pattern replication. The projection lens, tasked with focusing the light onto the wafer, requires stringent measures to remain free from contaminants, thereby ensuring the integrity of the image. Furthermore, The immersion liquid, integral to immersion lithography for enhancing resolution, must be maintained in a pristine state to avert any contamination that might compromise the photoresist. Additionally, rigorous cleaning of the wafer surface is essential to prevent the introduction and propagation of defects throughout the manufacturing process.

4.1 Contaminant control on photomask

The photomask is processed in the manufacturing process, cleaning procedure, machinery movement and high energy radiation, haze (precipitate) forms and grows even on defect-free masks. These contaminants, which can be organic, inorganic, or a hybrid type of both, may facilitate the crystal growth, leading to the decrease of transmittance, increase of scattered light and poor pattern formation. Meanwhile, Hyun et al. [85] have noted that the presence of particles on mask can disrupt pattern transfer under EUV exposure. Therefore, contaminants removal is a necessary step prior to mask exposure.

The main components of haze are carbon and sulfur, which are generated from atmosphere, residual photoresist or sulfate residue from photomask manufacturing process [86]. To reduce contaminants, Venkatesh et al. [87] have identified several cleaning techniques that effectively remove particles from photomasks, including megasonic cleaning, jet spray and aerosol cleaning. Megasonic cleaning with ozonated water enables to remove the organic contaminants and prevent the oxidation of metal layer on the photomask without side effect of chemical residue, compared to Piranha solution. As shown in Figure 7(a), Kindt et al. [88] compared the removal efficiency of three cleaning methods, including sulfuric peroxide mixture (SPM), ozone based process and one resist stripping process with the ozone and cryogenic cleaning. TOF-SIMS data reveals that sulfate-related compounds have been reduced significantly, but cannot achieve 100% removal. EUV mask cleaning is much more difficult than ArF mask, because the removal of contaminants and surface damage reduce the reflectivity through altering the oxidation and the roughness of the surface [9, 89]. Sometime EUV systems incorporate in-situ cleaning techniques, such as plasma or UV cleaning, to actively remove contaminants from critical surfaces without dismantling the system. Besides that, pellicles are ultra-thin particle filter designed to protect the mask from defects in DUV and EUV lithography, while the lifetime of pellicles membrane caused by heat from exposure is an extra concern [90].

4.2 Contaminant control in immersion flow field

Contaminants in immersion liquid encompass particles, metal ions, organic compounds and small molecules. To address these issues, an integrated purification system is typically linked with the liquid supply and recovery systems (Figure 1(b)). This system includes filters, heat control systems

For Review Only

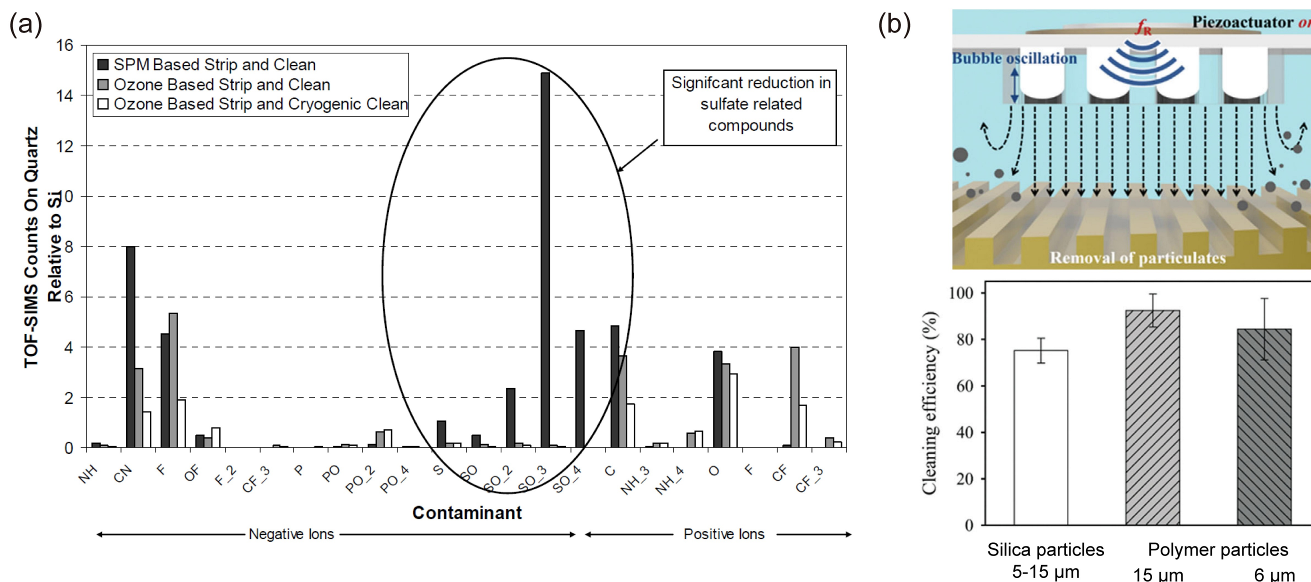

Figure 7 (a) Variable ions on a photomask are cleaned by three methods. Level of chemicals was measured by using TOF-SIMS [88]. (b) A schematic of a jet flow created by bubble oscillation to remove particulate contaminants from semiconductor wafer surfaces. Polymer are carboxy-modified acrylate-based polymer. Spacing of Grooves on contaminated wafer surface is around 500 μm [97].

and drainage to ensure the immersion liquid remains purified. To mitigate the adverse effects of soluble organic compounds, such as photoacid generators (PAGs), several solutions have been proposed. These include the development of novel photoresist formulations, the utilization of fluid degassing systems, and the optimization of tool and showerhead designs [91].

The primary contaminants in the immersion liquid are mainly suspended particles. Understanding the properties of these substances aids to their control and elimination. Even in pure water, a significant amount of pollutants can exist [92, 93]. These contaminants, acting as surface-active substances, can stabilize surface and bulk nanobubbles [94]. That means both particles and nanobubbles suspended in the immersed flow make the contaminate removal more difficult. For purifying the outflow of immersion liquid, integrated methods such as flocculation and centrifugation are employed to remove contaminants. Therefore, it is crucial to carefully analyze the sources of pollutants and the operation conditions to maintain uniformity in the submerged flow field.

4.3 Contamination control on wafer surface

The potential contaminants on the wafer surface include particles, metals, organic compounds, non-volatile residues, and moisture. To address these contaminants, rinsing with ozonized water is effective, and dilute hydrofluoric acid (DHF) can remove organics by lifting off the native oxide layer on the silicon substrate [95]. Reinhardt et al. [96] have extensively summarized various technologies for wafer rinsing, drying and storage.

Several innovative strategies have been proposed to control wafer surface contamination. For instance, Kim et al. [97] introduced a cleaning method to remove particles from the wafer surface using a jet flow composed of oscillating bubbles subjected to acoustic excitation. This technique effectively removes silica and polymer particles from wafers with micro-scale patterns, achieving a cleaning efficiency of over 75% for three types of particles (Figure 7(b)). However, this method's effectiveness in removing contaminants from nanostructures remains to be determined.

Additionally, Mertens et al. [98] developed a gas lock system for extreme ultraviolet (EUV) lithography, where the projection optics box is isolated from the wafer box by a conical tube. The cross-sectional area of this tube can be modeled to match the shape of the EUV beam, reducing hydrocarbon contamination by five orders of magnitude and achieving 5% EUV absorption. This separated design for wafer and optics significantly mitigates debris contamination.

Recently, the Leidenfrost droplet is demonstrated to be employed as an effective tool to remove the sticky particles within the microstructures [99], as shown in Figure 8(a). However, we should note that the presence of solid contaminants can affect the local evaporation rate of the droplet, and further influence the final fate of a Leidenfrost droplet [100], resulting in the explosion of the droplet (Figure 8(b)). Even the presence of chemical contamination can substantially change the behaviors of a Leidenfrost droplet. For example, the explosion of the droplet is also reported within a

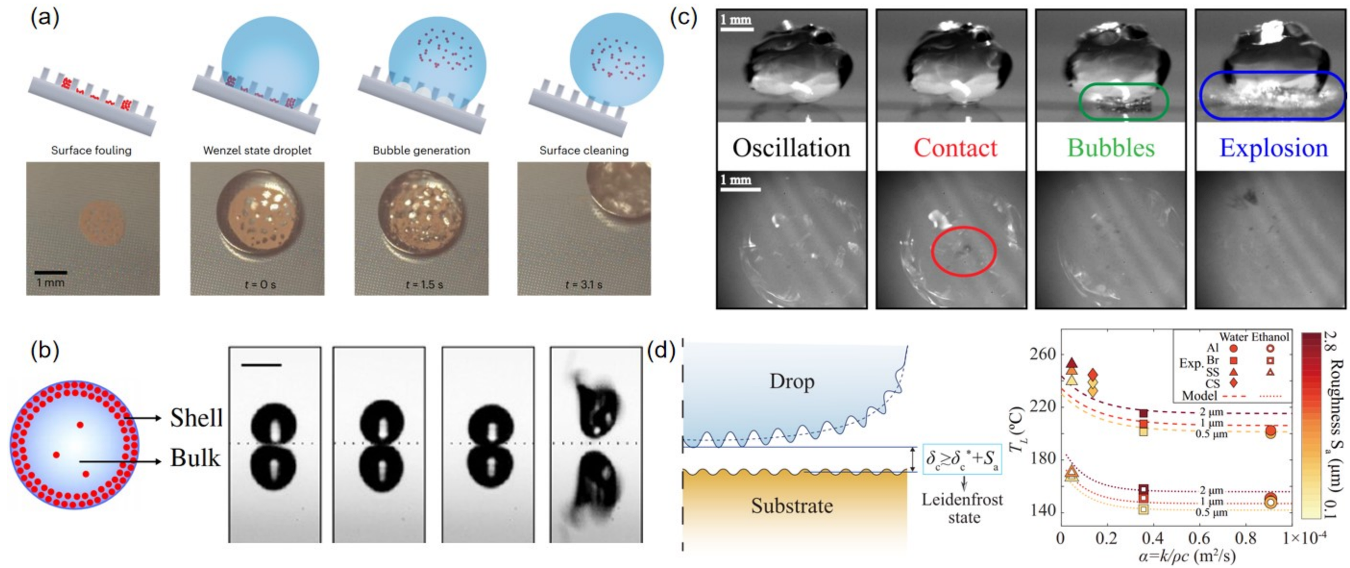

Figure 8 (a) Surface deep fouling removal by a Leidenfrost droplet [99]. (b) Explosion of a Leidenfrost droplet with the presence of particle contaminants [100]. (c) Explosion of a multicomponent Leidenfrost droplet [101]. (d) The effect of surface roughness on Leidenfrost temperature [102].

tricomponent Leidenfrost droplet [101] (Figure 8(c)), consisting of water, ethanol and oil. Moreover, the roughness of the microstructured surface is found to significantly influence the vapor film thickness underneath the Leidenfrost droplet, which can further affect the Leidenfrost temperature [102] (Figure 8(d)) and the droplet motion [103].

5 Conclusions

To summary, this review systematically addresses the challenges and advancements in photolithography, with a particular focus on characterizing and removing contaminants in deep ultraviolet and extreme ultraviolet lithography. The analysis underscores the critical importance of managing contaminants such as droplet, bubble, particle and chemical contaminants to maintain the integrity of photolithographic processes.

We listed a range of detection and analytical methods, including NTA, DLS, SEM, TOF-SIMS, dynamic SIMS, ICP-MS, Raman spectroscopy, XPS, and FTIR, which offer valuable insights into the nature and dynamics of these contaminants. These methods are pivotal in identifying and understanding contaminants at a granular level, thus facilitating more effective contamination control strategies.

Furthermore, the review discusses various approaches to controlling and mitigating contamination effects. Key strategies include the purification of critical components such as photomasks, immersion fluids, and wafer surfaces. Innovations in cleaning techniques, along with improvements in the purity of immersion fluids and the maintenance of wafer surfaces, are essential for advancing the capabilities of traditional photolithography.

This comprehensive examination of contamination control not only highlights current best practices but also points to future directions for research and development. Especially, understanding of fluid dynamic of interaction between droplet, bubble and particle either in the bulk or on the surface helps avoid the formation of contamination. By continually refining these aspects, the photolithography field can push the boundaries of resolution and efficiency, paving the way for the next generation of semiconductor manufacturing.

6 References

This work is supported by National Natural Science Foundation of China under Grants Nos. 11988102 and 12202244, the National Key R&D Program of China under Grant No. 2021YFA0716201, the New Cornerstone Investigator Program, the Xplorer Prize and Shuimu Scholarship at Tsinghua University (2024SM049, 2023SM038).

Conflict of interest The authors declare that they have no conflict of interest.

1 Y. Fang, and Y. He, J. Phys. Conf. Ser., 2221, 1, 012041 (2022).
2 L. Van den Hove, Metrology, Inspection, and Process Control XXXVI. PC12053 (2022).
3 G. E. Moore, Proc. IEEE, 86, 1, 82 (1998).
4 D. Burg, and A. Jesse H, PloS one 16, 8, e0256245 (2021).
5 K. Ronse, Microelectron. Eng., 100263 (2024).
6 H. J. Levinson, SPIE press, 146 (2005).
7 P. Graeupner, P. Kuerz, T. Stammler, J. Schoot, J. Stoeldraijer, In Optical and EUV Nanolithography. 12051, 1205102, SPIE (2022).
8 I. Lee, F. Joern-Holger, P. Vicky, R. Kurt, D. G. Stefan. and H. Eric, J. Micro/Nanopatterning Mater. Metrol. (2023).

For Review Only

1
2
3
4
5
6
7
8
9
10
11
12
13
14
15
16
17
18
19
20
21
22
23
24
25
26
27
28
29
30
31
32
33
34
35
36
37
38
39
40
41
42
43
44
45
46
47
48
49
50
51
52
53
54
55
56
57
58
59
60

9 R. P. Venkatesh, K. Min-Su, and P. Jin-Goo, Developments in Surface Contamination and Cleaning: Methods for Surface Cleaning, 135 (2017).
10 W. S. Meng, C. B. Zhao, J. Z. Wu, B. F. Wang, Q. Zhou, and K. L. Chong, Phys. Fluids, 36, 2 (2024).
11 M. Museau, M. Cédric, and T. Serge, Int J Interact Des Manuf, 127 (2007).
12 R. A. Lawson, A. P. Robinson, Front. nanotechnol., 11, 1 (2016).
13 Z. H. Wang, Y. L. Wu, D. F. Qi, W. H. Yu, and H. Y. Zheng, J. Opt., 24, 3, 033001 (2022).
14 I. Giannopoulos, I. Mochi, M. Vockenhuber, Y. Ekinci & D. Kazazis, arXiv preprint arXiv:2402.18234 (2024).
15 T. C. Wang, J. Phys. Conf. Ser., 2608, 1, 012016 (2023).
16 M. Totzeck, W. Ulrich, A. Göhnermeier, and W. Kaiser, Nat. Photonics, 1, 11, 629 (2007).
17 S. Owa, and H. Nagasaka, Lithography Asia 2008, 7140, 265 (2008).
18 M. McCallum, M. Kameyama, and S. Owa, Microelectron. Eng., 83, 4, 640 (2006).
19 X. Fu, Y. Huang, L. Hu, H. B. Xie, and W. Y. Chen, Flow Meas. Instrum., 53, 190 (2017).
20 R. M. M. Hasan, and X. Luo, Nanomanufacturing Metrol., 1, 67 (2018).
21 D. Lohse, Phys. Rev. Fluids, 3, 11, 110504 (2018).
22 D. P. Sanders, Chem. Rev., 110, 1, 321 (2010).
23 B. J. Rice, In Nanolithography, Woodhead Publishing, 42 (2014).
24 E. Sharma, R. Rathi, J. Misharwal, B. Sinhmar, S. Kumari, J. Dalal, and A. Kumar, Nanomaterials, 12, 16, 2754 (2022).
25 C. Wagner, and N. Harned, Nat. Photonics, 4, 1, 24 (2010).
26 S. Fujioka, H. Nishimura, K. Nishihara, N. Miyanaga, Y. Izawa, K. Mima, Y. Shimada, and A. Sunahara, Plasma and Fusion Research, 4, 048 (2009).
27 N. Lin, W. Yang, Y. Chen, X. Wei, C. Wang, J. Zhao, Y. Peng, and Y. Leng, Laser & Optoelectronics Progress, 59, 9, 0922002 (2022).
28 G. Zhu, Z. H. Xu, Y. Jin, X. Chen, L. J. Yang, J. Xu, D. B. Shan, Y. B. Chen, and B. Guo, Opt. Lasers Eng., 157, 107130 (2022).
29 Y. Y. Wei, S. Brandl, and F. Goodwin, In Advances in Resist Materials and Processing Technology XXV, 6923, 610 (2008).
30 J. Mulkens, B. Streefkerk, H. Jasper, J. de. Klerk, F. de. Jong, L. Levasier, and M. Leenders, In Optical Microlithography XX, 6520, 75 (2007).
31 D. Lohse, and X. H. Zhang, Nat. Rev. Phys. 2, 8, 426 (2020).
32 J. H. Snoeijer, and B. Andreotti, Annu. Rev. Fluid Mech., 45, 1, 269 (2013).
33 Y. Liu, and X. Zhang, J. Chem. Phys., 138, 1 (2013).
34 D. Lohse, and X. H. Zhang, Phys. Rev. E., 91, 3, 031003 (2015).
35 A. L. Yarin, Annu. Rev. Fluid Mech., 38, 1, 159 (2006).
36 X. Cheng, T. P. Sun, and L. Gordillo, Annu. Rev. Fluid Mech., 54, 1, 57 (2022).
37 C. Josserand, and S. T. Thoroddsen, Annu. Rev. Fluid Mech., 48, 1, 365 (2016).
38 L. Xu, W. W. Zhang, and S. R. Nagel, Phys. Rev. Lett., 94, 18, 184505 (2005).
39 S. T. Thoroddsen, T. G. Etoh, K. Takehara, N. Ootsuka, and Y. Hatsuki, J. Fluid Mech., 545, 203 (2005).
40 T. Niiyama, and A. Kawai, JPN J APPL PHYS., 45, 5383 (2006).
41 B. He, and A. A. Darhuber, Colloids Surf. A., 583, 123912 (2019).
42 Y. Wakata, X. Chao, C. Sun, and C. Diddens, J. Fluid Mech., 984, A17 (2024).
43 H. Zeng, Y. Wakata, X. Chao, M. B. Li and C. Sun, J. Colloid Interface Sci., 648, 736 (2023).
44 J. H. Weijs, B. Andreotti, and J. H. Snoeijer, Soft Matter, 9, 35, 8494 (2013).
45 C. S Chen, H. G Zhang, and X. R. Zhang, Commun. Theor. Phys., 75, 12, 125504 (2023).
46 Q. Yang, P. Z. Sun, L. Fumagalli, Y. V. Stebunov, S. J. Haigh, Z. W. Zhou, I. V. Grigorieva, F. C. Wang, and A. K. Geim, Nature, 588, 7837, 250 (2020).
47 D. Seveno, T. D. Blake, and J. De Coninck, Phys. Rev. Lett. 111, 9, 096101 (2013).
48 J. Fan, J. De Coninck, H. Wu, and F. Wang, Phys. Rev. Lett., 124, 12, 125502 (2020).
49 S. Chen, Z. J. Guo, H. G. Zhang, I. Pagonabarraga, and X. R. Zhang, Eur. Phys. J., 45, 7, 60 (2022).
50 Y. T. Cheng, K. C. Chu, H. K. Tsao, and Y. J. Sheng, J. Colloid Interface Sci., 578, 69 (2020).
51 A. Kawai, T. Niiyama, H. Endo, M. Yamanaka, A. Ishikawa, K. Suzuki, O. Tamada, and M. Sanada, In Advances in Resist Technology and Processing XXIII, 6153, 594 (2006).
52 C. H. Lin, and L. A. Wang, J. Vac. Sci. Technol. B, 23, 6, 2684 (2005).
53 H. B. Burnett, A. C. Wei, M. S. El-Morsi, T. A. Shedd, G. F. Nellis, C. Van Peski and A. Grenville, J Micro Nanolithogr MEMS MOEMS, 5, 1, 013008 (2006).
54 A. Azevedo, H. Oliveira, and J. Rubio, Adv. Colloid Interface Sci, 271, 101992 (2019).
55 E. P. Favvas, G. Z. Kyzas, E. K. Efthimiadou, and A. C. Mitropoulos, Curr. Opin. Colloid Interface Sci, 54, 101455 (2021).
56 X. T. Ma, M. B. Li, P. Pfeiffer, J. Eisener, C. D. Ohl, and C. Sun, J. Colloid Interface Sci., 606, 1380 (2022).
57 M. Alheshibri, J. Qian, M. Jehannin and V. S. Craig, Langmuir, 32, 43, 11086 (2016).
58 N. Nirmalkar, A. W. Pacek, and M. Barigou, Langmuir, 34, 37, 10964 (2018).
59 M. R. Ghaani, P. G. Kusalik, and N. J. English, Sci. Adv., 6, 14, eaaz0094 (2020).
60 X. T. Ma, M. B. Li, and C. Sun, J. Hydrol., 34, 6, 1121 (2022).
61 M. B. Li, Y. Wakata, H. Zeng, and C. Sun, J. Colloid Interface Sci., 652, 1944 (2023).
62 X. T. Ma, M. B. Li, X. F. Xu. and C. Sun, Appl. Surf. Sci., 608, 155232 (2023).
63 M. B. Li, X. T. Ma, J. Eisener, P. Pfeiffer, C. D. Ohl, and Sun, C, J. Colloid Interface Sci., 596, 184 (2021).
64 M. B. Li, L. Yi, and C. Sun, J. Colloid Interface Sci., 628, 223 (2022).
65 Y. W. Gao, K. Francis, and X. H. Zhang, Food Res Int, 157, 111246 (2022).
66 C. S. Chen, X. R Zhang, and D. P. Cao, GEE, 5, 374 (2020).
67 M. Alheshibri, M. Jehannin, V. A. Coleman, and V. S. Craig, J. Colloid Interface Sci., 554, 388 (2019).
68 A. J. Jadhav, and M. Barigou, Langmuir, 36, 7, 1699 (2020).
69 A. M. Jaramillo-Granada, A. D. Reyes-Figueroa, and J. C. Ruiz-Suárez, Phys. Rev. Lett., 129, 9, 094501 (2022).
70 J. Qiu, Z. L. Zou, S. Wang, X. Y. Wang, L. Wang, Y. M. Dong, H. W. Zhao, L. J. Zhang, and J. Hu, ChemPhysChem, 18, 10, 1345 (2017).
71 F. Eklund, and J. Swenson, Langmuir, 34, 37, 11003 (2018).
72 Z. Gao, W. X. Wu, W. T. Sun, and B. Wang, Langmuir, 37, 38, 11281 (2021).
73 P. C. Zhang, C. S. Chen, M. Y. Feng, C. Sun, and X. F. Xu, J. Am. Chem. Soc., 146, 28, 19537 (2024).
74 Q. X. Xiao, Y. W. Liu, Z. J. Guo, Z. P. Liu, and X. R. Zhang, Appl. Phys. Lett., 111, 13, (2017).
75 M. Terai, T. Ishibashi, T. Hagiwara, T. Hanna, T. Kumada, Y. Takebe, O. Yokokoji, T. Fujiwara, J. Jiang, T. Niwa, and S. Wakamizu, J. Photopolym. Sci. Technol., 21, 5, 665 (2008).
76 T. Tamura, N. Onoda, M. Fujita, and T. Uchiyama, In Optical Microlithography XXI, 6924, 442 (2008).
77 N. Takahashi, S. Shimura, and T. Kawasaki, In Advances in Resist Materials and Processing Technology XXIV, 6519, 642 (2007).
78 S. Kusumoto, M. Shima, Y. Wang, T. Shimokawa, H. Sato, and K.Hieda, Polymer.Adv.Tech., 17, 2, 122 (2006).
79 M. Sado, T. Teratani, H. Fujii, R. Iikawa, and H. Iida, Appl. Surf. Sci., 255, 4, 1018 (2008).

For Review Only

1 2 3 4 5 6 7 8 9 10 11 12 13 14 15 16 17 18 19 20 21 22 23 24 25 26 27 28 29 30 31 32 33 34 35 36 37 38 39 40 41 42 43 44 45 46 47 48 49 50 51 52 53 54 55 56 57 58 59 60

80 S. Eswara, A. Pshenova, L. Yedra, Q. H. Hoang, J. Lovric, P. Philipp, and T. Wirtz, Appl. Phys. Rev., 6, 2 (2019).

81 R. Varanasi, M. Mesawich, P. Connor, and L. Johnson, In Advances in Patterning Materials and Processes XXXIV, 10146, 462 (2017).

82 P. H. Chi, F. H. Ko, C. T. Hsu, H. L. Chen, C. K. Yang, Y. C. Sun, and M. H. Yang, Anal. At. Spectrom., 17, 4, 358 (2002).

83 R. Nagarajan, S. Awad, and K. R. Gopi, In Developments in Surface Contamination and Cleaning, 31 (2011).

84 S. B. Zhu, In Metrology, Inspection, and Process Control for Microlithography XV, 4344, 589 (2001).

85 Y. Hyun, J. Kim, K. Kim, S. Koo, S. Kim, Y. Kim, C. Lim, and N. Kwak, In Extreme Ultraviolet (EUV) Lithography VI, 9422, 605 (2015).

86 S. J. Han, S. Y. Yu, M. G. Sung, Y. H. Kim, H. S. Yoon, and J. M. Sohn, In Photomask and Next-Generation Lithography Mask Technology X, 5130, 563 (2003).

87 J. S. Papanu, R. Gouk, H. W. Chen, P. Boelen, P. Peters, M. Belisle, S. Verhaverbeke, A. Ko, K. Child, and E. In 22nd European Mask and Lithography Conference, 6281, 192 (2006).

88 L. Kindt, A. Watts, J. Burnham, and W. Aaskov, In Photomask Technology 2006, 6349, 439 (2006).

89 F. Eschbach, P. Coon, B. Greenebaum, A. Mittal, P. Sanchez, D. Tanzil, G. Ng, H. Yun, and A. Sengupta, In Photomask and Next-Generation Lithography Mask Technology XII, 5853, 74 (2005).

90 E. S. Park, M. H. Kim, S. Hwang, and H. K. Oh, Microelectron. Eng., 177, 74 (2017).

91 H. Lee, S. Park, M. Kim, J. Moon, B. Lee, and M. Cho, J. Mater. Chem. C, 9, 4, 1183 (2021).

92 I. Schlesinger, and U. Sivan, J. Am. Chem. Soc., 140, 33, 10473 (2018).

93 C. S. Chen, H. G. Zhang, and X. R. Zhang, Commun. Theor. Phys., 75, 12, 125504 (2023).

94 H. G. Zhang, S. Chen, Z. J. Guo, X. R. Zhang, Phys. Chem. Chem. Phys., 24, 9685 (2022).

95 T. Hattori, AIP Conf. Proc., 550, 1, 275 (2001).

96 K. Reinhardt, and K. Werner, Handbook of silicon wafer cleaning technology, William Andrew (2018).

97 D. Kim, J. Hong, and S. K. Chung, Korean J. Chem. Eng., 39, 12, 3261 (2022).

98 B. M. Mertens, B. Van der Zwan, P. W. H. De Jager, M. Leenders, H. G. C. Werij, J. P. H. Benschop, and A. J. J. Van Dijsseldonk, Microelectron. Eng., 53, 659 (2000).

99 W. G. Huang, L. Zhao, X. K. He, Y. Li, C. P. Collier, Z. Zheng, J. S. Liu, D. P. Briggs, and J. T Cheng, Nat. Phys., 1 (2024).

100 S. J. Lyu, V. Mathai, Y. Wang, B. Sobac, P. Colinet, D. Lohse, and C. Sun, Sci. Adv., 5, 5, eaav8081 (2019).

101 S. J. Lyu, H. Tan, Y. Wakata, X. Yang, C. K. Law, D. Lohse, and C. Sun, PNAS, 118, 2, e2016107118 (2021).

102 Y. Wakata, N. Zhu, X. L Chen, S. J. Lyu, D. Lohse, X. Chao, and C. Sun, Phys. Rev. Fluids, 8, 6, L061601 (2023).

103 A. Li, H. Z. Li, S. J. Lyu, Z. P. Zhao, L. L. Xue, Z. Li, K. X. Li, M.Z. Li, C. Sun & Y. L. Song, Nat. Commun., 14, 1, 2646 (2023).

For Review Only